Phosphorus-Based Ambidentate Chelating Ligands: Pyridyl-*N*− and Imido-*N*−Metal Coordination in the $Py_2P(NSiMe_3)_2$ Anion

Stefan Wingerter,[†] Matthias Pfeiffer,[†] Alexander Murso,[†] Christian Lustig,[†] Thomas Stey,[†] Vadapalli Chandrasekhar,[‡] and Dietmar Stalke*[,†]

Contribution from the Institut für Anorganische Chemie der Universität Würzburg, Am Hubland, D-97074 Würzburg, Germany, and Indian Institute of Technology, Kanpur, Department of Chemistry, Kanpur-208 016, India

Received June 30, 2000

Abstract: Monoanionic heteroallylic ligand systems [R−N−E−N−R]$^-$ (E = Si(R_2), S(R_2) or S(R), C(R), and P(R_2)) are versatile chelating substituents both in main group and transition metal chemistry as they provide sufficient steric demand and solubility to the products. Their application is only limited by the rigid bite of the ligands as the N···N distance cannot be tuned to the various radii of different metals. In this paper we present the new concept of opening the ligand periphery to additional coordination. The NP(R_2)N$^-$ chelate in classical aminoiminophosphoranates is extended by additional coordination sites in the organic substituents (e.g., 2-pyridyl (Py) instead of phenyl (Ph)). $Py_2P\{N(H)SiMe_3\}(NSiMe_3)$ (**1**) is the starting material for a new class of complexes as deprotonated **1** contains along with the NPN$^-$ chelate the pyridyl ring nitrogen atoms to generate a side-selective Janus face ligand. In $[(THF)Sr\{Py_2P(NSiMe_3)_2\}_2]$ (**2**) and $[(4,4'\text{-bipy})Ba\{Py_2P(NSiMe_3)_2\}_2]_n$ (**3**) both pyridyl rings are involved in metal coordination but only one imido nitrogen atom. Hence, the classical NP(Ph_2)N$^-$ chelating ligand is converted into a NP(Py_2)N$^-$ tripodal ligand. In the coordination to zinc in the complex $[Zn\{Py_2P(NSiMe_3)_2\}_2]$ (**4**) one pyridyl ring and one imido nitrogen atom is employed in metal coordination. Pyridyl substitution of the P(V) center gives not only access to new coordination modes but also changes the reactivity of aminoiminophophoranes considerably. $[Li(Py_2PNSiMe_3)]_2$ (**5**) is a lithiated phosphanylamine derived from the reduction of **1** with lithium di(trimethylsilyl)amide. Reaction of **1** with lithium organics yields $[(THF)_2Li(Py_2P)]$ (**6**). Pyridyl substitution facilitates single or even double P═N bond cleavage, unprecedented in alkyl- or aryl-substituted aminoiminophosphoranes. This reduction of P(V) species to P(III) compounds supplies easy access to phosphanylamines and secondary phosphanes.

Introduction

A principal strategy in synthetic inorganic and organometallic chemistry is the employment of tailor-made ligand systems to create metal complexes of specific nuclearity, coordination number, geometry, and reactivity.[1] Typical functions of such ligands are to inhibit oligomerization reactions, to stabilize the low valent form and/or the low oxidation state of the metal center, and to model the shape of the complex periphery. These ligands need to provide significantly high flexibility since metal centers of soft and hard Lewis acidity require to be complexed each in the most suitable fashion. In addition to the capability to delocalize electron density, a multifunctional ligand should have a geometric adaptability as well, that is, it should be variable enough to accommodate metal centers which are different in size within a moderate range. The so-called scorpionates can be considered to be the archetype of these self-adapting chelates or tripodal ligands.[2]

Monoanionic heteroallylic ligand systems [R−N−E−N−R]$^-$ with E = Si(R_2),[3] S(R_2) or S(R),[4] C(R),[5] and P(R_2)[6] are of similar interest as versatile chelating ligands. Of these the aminoiminophosphoranates $[Me_3Si-N-P(R_2)-N-Me_3Si]^-$ deserve special mention.[7] These ligands are derived formally by the deprotonation of $R_2P(NSiMe_3)(NHSiMe_3)$. The resulting chelating ligand is comparable in terms of its cone angle to the

[†] Universität Würzburg.
[‡] Indian Institute of Technology.

(1) Review: Kottke, T.; Stalke, D. *Chem. Ber./Recl.* **1997**, *130*, 1365.

(2) (a) Trofimenko, S. *Prog. Inorg. Chem.* **1986**, *34*, 115. (b) Trofimenko, S. *Chem. Rev.* **1993**, *93*, 943. (c) Kitajima, N.; Tolman, W. B. *Prog. Inorg. Chem.* **1995**, *43*, 419.

(3) Review: (a) Veith, M. *Angew. Chem.* **1987**, *99*, 1; *Angew. Chem., Int. Ed. Engl.* **1987**, *26*, 1. (b) Veith, M.; Böhnlein, J. *Chem. Ber.* **1989**, *122*, 603. (c) Veith, M.; Böhnlein, J.; Huch, V. *Chem. Ber.* **1989**, *122*, 841.

(4) Review: (a) Fleischer, R.; Stalke, D. *Coord. Chem. Rev.* **1998**, *176*, 431 and ref. therein. (b) Pauer, F.; Rocha, J.; Stalke, D. *J. Chem. Soc. Chem. Commun.* **1991**, 1477. (c) Fleischer, R.; Freitag, S.; Pauer, F.; Stalke, D. *Angew. Chem.* **1996**, *108*, 208; *Angew. Chem., Int. Ed. Engl.* **1996**, *35*, 204. (d) Fleischer, R.; Rothenberger, A.; Stalke, D. *Angew. Chem.* **1997**, *109*, 1140; *Angew. Chem., Int. Ed. Engl.* **1997**, *36*, 1105. (e) Fleischer, R.; Walfort, B.; Gbureck, A.; Scholz, P.; Kiefer, W.; Stalke, D. *Chem. Eur. J.* **1998**, *4*, 2266.

(5) (a) Fenske, D.; Hartman, E.; Dehnicke, K. *Z. Naturforsch.* **1988**, *43B*, 1611. (b) Ergezinger, C.; Weller, F.; Dehnicke, K. *Z. Naturforsch.* **1988**, *43B*, 1621. (c) Maier, S.; Hiller, W.; Strähle, J.; Ergezinger, C.; Dehnicke, K. *Z. Naturforsch.* **1988**, *43B*, 1628. (d) Hey, E.; Ergezinger, C.; Dehnicke, K. *Z. Naturforsch.* **1989**, *44B*, 205. (e) Stalke, D.; Wedler, M.; Edelman, F. T. *J. Organomet. Chem.* **1992**, *431*, C1. (f) Westerhausen, M.; Hausen, H.-D. *Z. Anorg. Allg. Chem.* **1992**, *615*, 27. (g) Westerhausen, M.; Schwarz, W. *Z. Naturforsch., B: Chem. Sci.* **1992**, *47*, 453. (h) Westerhausen, M.; Hausen, H.-D.; Schwarz, W. *Z. Anorg. Allg. Chem.* **1992**, *618*, 121. (i) Westerhausen, M.; Schwarz, W. *Z. Anorg. Allg. Chem.* **1993**, *619*, 1455.

(6) (a) Roesky, H. W. In *The Chemistry of Inorganic Ring Systems; Studies in Inorganic Chemistry*; Steudel, R., Ed.; Elsevier: Amsterdam, 1989. (b) Review: Witt, M.; Roesky, H. W. *Chem. Rev.* **1994**, *94*, 1163. (c) Review: Edelmann, F. T. *Top. Curr. Chem.* **1996**, *179*, 114.

(7) (a) Roesky, H. W.; Katti, K. V.; Seseke, U.; Witt, M.; Egert, E.; Herbst, R. Sheldrick, G. M. *Angew. Chem.* **1986**, *98*, 447; *Angew. Chem., Int. Ed. Engl.* **1986**, *25*, 477. (b) Hasselbring, R.; Roesky, Noltemeyer, M. *Angew. Chem.* **1992**, *104*, 613; *Angew. Chem., Int. Ed. Engl.* **1992**, *31*, 601. (c) Bachert, I.; Braunstein, P.; Guillon, E.; Massera, C.; Rose, J.; Decian, A. Fischer, J. *J. Cluster Sci.* **1999**, *10*, 445.

10.1021/ja0023736 CCC: $20.00
Published on Web 01/30/2001

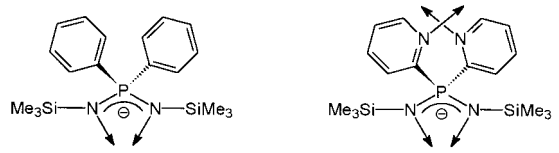

Figure 1. Substitution of the two phenyl rings in the chelating aminoiminophosphoranate monoanion (left) by pyridyl rings converts the chelate into a multifunctional Janus face ligand (right).

ubiquitous $C_5Me_5^-$ ligand.[8] By variation of the P-bonded organic groups specific properties of the corresponding metal complexes can be tuned sterically (i.e., via modification of the cone angle of the ligand) and electronically. The presence of silylated substituents on nitrogen ensures solubility as well as steric protection to the coordinated metal ion. These desirable features have enabled the use of these ligands as building blocks for many transition and main group metal-containing metallacycles.[6,7] Further modification of the compounds is possible by invoking the reactivity of the N−$SiMe_3$ group. Thus, in its coordination behavior toward alkali[9] and alkaline earth metal[10] ions the chelating $[Ph_2P(Me_3SiN)_2]$ bidentate anion provides sufficient bulk to prevent the metal complexes from aggregation. The ready solubility of these complexes in organic solvents including nonpolar hydrocarbons allowed their controlled conversion to gels of the formula $M(OH)_2 \cdot xH_2O$ (M = Be, Mg, Ca, Sr, Ba).[11]

The versatility of the above ligand systems can be enhanced by the construction of additional coordinating sites separated away from the anionic center. Thus, the incorporation of the pyridyl substituents on the phosphorus center in the place of the phenyl groups alters and augments the coordination capability of the ligand system and leads to the design of multi-dentate *Janus faced* ligands (Figure 1).

Different to the simple aminoiminophosphoranate anions the pyridyl derivatives would have two potential chelating sites, first the $[N-P-N]^-$ skeleton, predominantly accommodating the negative charge, and second the two remote nitrogen atoms in the pyridyl substituents. However, free rotation about the $P-C_{ipso}$ bond can easily bring the pyridyl nitrogen atoms into a more proximal and convenient location for coordination. An additional possibility of a π-interaction of the heteroaromatic ring to the metal also exists. To test these ideas we have designed and assembled the first example of a pyridyl-substituted aminoiminophosphoranate type of ligand. The varied coordination behavior of this ligand toward alkaline earth metal ions vis-á-vis Zn^{2+} ion is described. Besides, we also describe interesting facets of the reactivity of this ligand toward organolithium reagents wherein we observe a remarkable P═N bond cleavage.

Results and Discussion

Synthesis of 1, 2, 3, and 4. The synthesis of $Py_2P\{N(H)SiMe_3\}(NSiMe_3)$ (**1**) is carried out as detailed in Scheme 1 in analogy to the diphenyl-substituted derivative.[12] A Staudinger reaction of di(2-pyridyl)phosphane with 2 equiv of trimethylsilyl azide over a prolonged period affords a crude solid from which compound **1** can be obtained in a pure form first by distillation and later by crystallization. The ^{31}P NMR spectrum for this compound shows a single resonance at −6.2 while the ^{29}Si NMR spectrum shows two signals at 6.6 and 7.3, respectively. The characteristic ν(P═N) is seen at 1194 cm^{-1}. The structure of this compound was further confirmed by an X-ray structure determination (vide infra).

Scheme 1

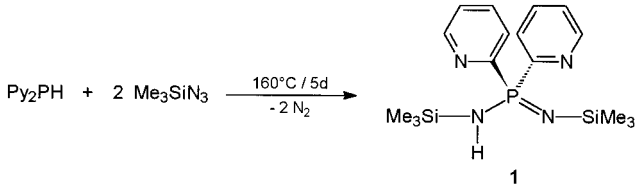

Compound **1** contains several reaction sites: (1) the acidic N−H functionality, (2) the imino nitrogen atom as a coordination site, (3) the pyridyl nitrogen atoms, and (4) the cleavage of the Si−N and P−N bonds.[13] From among all of these we have chosen to access the amino site as a convenient entry point to probe the reactivity of **1**. Deprotonation of the N−H group by a strong base would generate a chelating NPN-unit. Useful metal precursors for this purpose are either metal amides[14] or metal alkyls. Accordingly the reaction of **1** with $[M\{N(SiMe_3)_2\}_2]$ (M = Sr or Ba) proceeds quite smoothly at room temperature to afford the complexes $[(THF)Sr\{Py_2P(NSiMe_3)_2\}_2]$ (**2**) and $[(4-4'\text{-bipy})Ba\{Py_2P(NSiMe_3)_2\}_2]_n$ (**3**). In an analogous manner dimethylzinc reacts with **1**, and complete elimination of methane results in the formation of $[Zn\{Py_2P(NSiMe_3)_2\}_2]$ (**4**). These reactions are summarized in Scheme 2. The ^{31}P NMR spectra of the compounds **2**, **3**, and **4** show different trends in relation to **1**. Thus, while the chemical shift of the strontium derivative is strongly upfield-shifted (−15.9 ppm) those of the barium and zinc derivatives are much less affected and in fact move slightly downfield (−4.3 and −3.5 ppm, respectively). The compounds **2**−**4** are readily soluble in a large variety of organic solvents and can be crystallized from their solutions at subambient temperatures.

Reactivity of $[Py_2P(NSiMe_3)(NHSiMe_3)]$ (1) with Lithium Reagents and the Isolation of P−N Cleaved Compounds. The reactions of organolithium reagents or bis(trimethylsilyl)lithium amide with **1** proceed in an unexpected and entirely different manner in comparison to the reactions described above with alkaline earth or zinc reagents. The mechanism of these reactions is quite complex[15] and is not yet fully delineated.

In the reaction of **1** with the lithium amide $[(THF)LiN(SiMe_3)_2]$ compound **5** was isolated as the only product (Scheme 3). In this reaction a P−N bond is broken, and the phosphorus is reduced to an oxidation state three. The product isolated can be considered as the dimer of the lithium salt of di(2-pyridyl)-phosphino trimethylsilylamine. The ^7Li NMR of compound **5** shows a single resonance at 4.1 ppm. The equivalence of the phosphorus nuclei also in the compound **5** is confirmed by the observation of singlet at 15.3 ppm in the ^{31}P NMR. This value is considerably downfield-shifted in comparison to **1** as well as the complexes **2**, **3**, or **4**.

In a sharp contrast to the reaction pathway found above, the reaction of **1** with *n*-butyllithium or methyllithium leads to the

(8) Richter, J.; Edelmann, F. T.; Noltemeyer, M.; Schmidt, H.-G.; Shmulinson, M.; Eisen, M. S. *J. Mol. Catal., Sect. A* **1998**, *130*, 149.
(9) Steiner, A.; Stalke, D. *Inorg. Chem.* **1993**, *32*, 1977.
(10) Fleischer, R.; Stalke, D. *Inorg. Chem.* **1997**, *36*, 2413.
(11) Pandey, S. K.; Steiner, A.; Roesky, H. W.; Stalke, D. *Angew. Chem.* **1993**, *105*, 625; *Angew. Chem., Int. Ed. Engl.* **1993**, *32*, 596.
(12) Paciorek, K. L.; Kratzer, R. H. *J. Org. Chem.* **1966**, *31*, 2426.
(13) (a) Schmidbaur, H.; Schwirten, K., Pickel; H.-H. *Chem. Ber.* **1969**, *102*, 564. (b) Wolfsberger, W.; Hager, W. *Z. Anorg. Allg. Chem.* **1976**, *425*, 169. (c) Wolfsberger, W.; Hager, W. *Z. Anorg. Allg. Chem.* **1977**, *433*, 247.
(14) Westerhausen, M. *Inorg. Chem.* **1991**, *30*, 96. (b) Vaartstra, B. A.; Huffman, J. C.; Streib, W. E.; Caulton, K. G. *Inorg. Chem.* **1991**, *30*, 121.
(15) The reactiviy of the $Py_nPh_{3-n}P{=}NSiMe_3$, $n = 1, 2, 3$, with lithium organics or alkali metals, has been studied: Wingerter, S.; Pfeiffer, M.; Murso, A.; Steiner, A.; Chandrasekhar, V.; Stalke, D., unpublished results.

Scheme 2

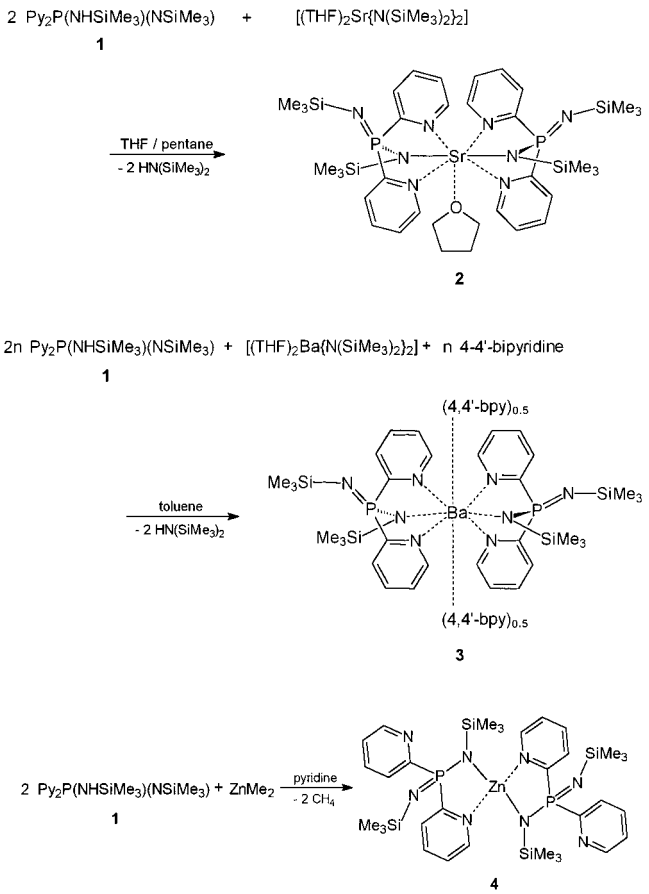

Scheme 3

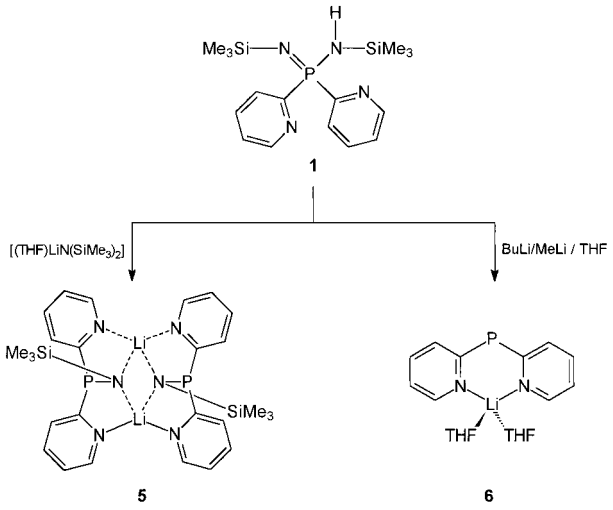

formation of the lithiumphosphide **6** (Scheme 3). This reaction is quite remarkable. While one-half of the ligand (N−P−N segment) undergoes bond scission involving the P−N bonds the other half of the ligand involving the Py−P−Py part remains unscathed. Phosphorus undergoes a reduction accompanying the cleavage of both the P═N and P−N bonds. The lithium phosphide **6** can be independently generated by the deprotonation of di(2-pyridyl)phosphane, Py_2PH with either *n*-butyllithium or methyllithium.[16a] Another route for the synthesis of compound **6** which we reported earlier is by a P−C bond cleavage of tri-(2-pyridyl)phosphane using lithium metal.[16b] Although the

(16) (a) Steiner, A.; Stalke, D. *Organometallics* **1995**, *14*, 2422. (b) Steiner, A.; Stalke, D. *J. Chem. Soc., Chem. Commun.* **1993**, 444.

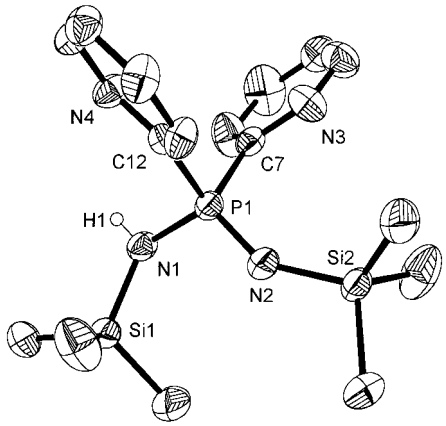

Figure 2. Solid-state structure of $Py_2P\{N(H)SiMe_3\}(NSiMe_3)$ (**1**). Anisotropic displacement parameters are depicted at the 50% probability level. Selected bond lengths [pm] and angles [deg] are presented in Table 1.

phosphorus atom is dicoordinate in **6**, its chemical shift value of 13.0 ppm is very similar to that observed for **5**. Nevertheless, cleavage of P−N bonds in the presence of organometallic reagents has been documented previously, particularly in the substitution reactions of halogenocyclophosphazenes[17] where the primary driving force for such reactions is the metal−halogen exchange reaction followed by the coordination of the metal ion by the nitrogen atoms of the ring; the type of reactivity seen in the present instance is completely unprecedented. Thus, for example, analogous reactions with $Ph_2P(NSiMe_3)(NHSiMe_3)$ proceed in a normal way with deprotonation without P−N bond scission and with the lithium ion being coordinated by the chelating NPN-unit.[9]

Crystal Structure of $[Py_2P(NSiMe_3)(NHSiMe_3)]$ (1). The N,N′-bis(trimethylsilyl)aminoiminodipyridylphosphorane **1** is obtained as a crystalline material from an oil that can be distilled out from the crude product. The molecular structure of **1** is shown in Figure 2.

The two P−N bond lengths present in this molecule are not equal with P1−N1 being 164.9(2) and P1−N2 being 152.9(2) pm. It is known that an average P−N single-bond distance in P(V) compounds is 170.0 pm.[18] Thus both the bond lengths observed are smaller than this value. It is instructive to compare the situation found in an analogous acyclic P−N compound, $[Ph_2PN(SiMe_3)PPh_2{=}NSiMe_3]$.[19] In this latter compound a shorter bond of 153.5(2) and a longer one of 169.3(2) pm (av) is observed. Also, the bond angles around the two nitrogen atoms in **1** point to their dissimilarity with each other. Thus, the Si1−N1−P1 angle is 123.10(10)°, whereas the corresponding angle at the imino nitrogen atom N2 is 146.89(11)°, suggesting that the hybridization at the latter has lesser p character than the former. The N1−H group in **1** interacts with a pyridyl nitrogen atom of an adjacent molecule leading to an interesting intermolecular hydrogen bonding in the form of N−H···N bridges. This results in the formation of a dimeric structure containing a ten-membered ring system (Figure 3).

The metric parameters involved in the hydrogen bonding are quite reasonable with the N1A−H1A distance of 80.7(2) and H1A···N4B distance of 247.3(2) pm. The N−H···N motif is

(17) (a) Allcock, H. R.; Desorcie, J. L.; Riding, G. H. *Polyhedron* **1987**, *6*, 119. (b) Chandrasekhar, V.; Justin Thomas, K. R. *Struct. Bonding* **1993**, *81*, 43.

(18) Rademacher, P. In *Strukturen Organischer Moleküle*; VCH: Weinheim, 1987.

(19) Braunstein, P.; Hasselbring, R.; Stalke, D. *New J. Chem.* **1996**, *20*, 337.

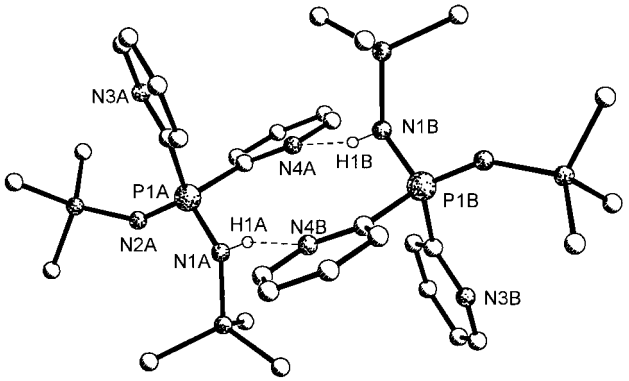

Figure 3. Solid-state arrangement of two molecules of $Py_2P\{N(H)SiMe_3\}(NSiMe_3)$ (**1**), showing mutual intermolecular hydrogen bonding.

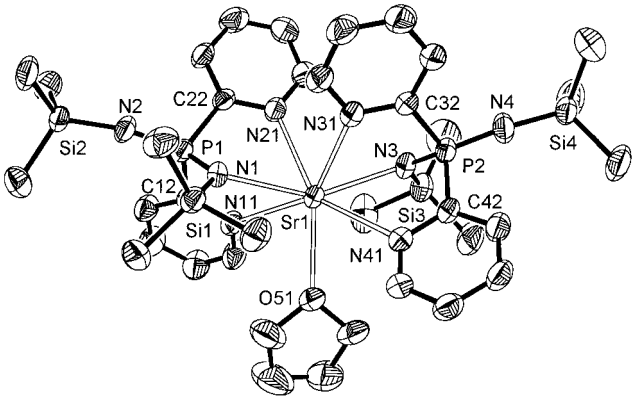

Figure 4. Solid-state structure of $[(THF)Sr\{Py_2P(NSiMe_3)_2\}_2]$ (**2**). Anisotropic displacement parameters are depicted at the 50% probability level. Selected bond lengths [pm] and angles [deg] are presented in Table 1.

fairly linear as evidenced by a bond angle of 153.11(2)°. These parameters are in keeping with the hydrogen-bonding trends known for N−H···N secondary interactions.[20]

X-ray Crystal Structure of $[(THF)Sr\{Py_2P(NSiMe_3)_2\}_2]$ (2). Single crystals of compound **2** have been obtained from a solution of THF/pentane at −18 °C. **2** is a monomer in the solid state (Figure 4).

Two molecules of deprotonated **1** are coordinated to the strontium ion in a tripodal k^3 mode. The amino hydrogen atom on each ligand reacts with the metal amide to form a M−N bond. The second imino nitrogen atoms of the ligand, on the other hand, do not interact with the metal ion. In contrast, however, *both* the pyridyl nitrogen atoms of each ligand are involved in coordination. Thus, the metal is enveloped by two molecules of ligand **1** with a coordination environment of four pyridyl nitrogen atoms and two amido nitrogen atoms in a tripodal fashion. A seventh coordination site is occupied by a solvent THF molecule.

The two tripodal chelating ligands coordinate to the strontium ion in nearly the same mode. In spite of this, however, within each ligand different Sr−N distances are found. The amido metal bonds (Sr1−N1 260.6(4) and Sr1−N3 259.3(4) pm) are the shortest nitrogen−metal distances found in this molecule. These distances are comparable to those observed earlier in $[(THF)_2Sr\{(NSiMe_3)_2PPh_2\}_2]$[10] (av 263.8 pm) or in $[(THF)_2Sr\{(NSiMe_3)_2CPh\}_2]$[5h] (259 pm) but longer than that found for $[(DME)_2Sr\{(NSiMe_3)_2\}_2]$[21] (244 pm). The two pyridyl rings of every ligand differ in their coordination to the metal center.

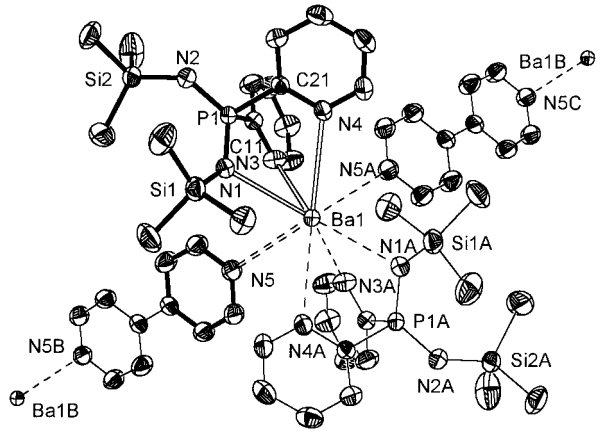

Figure 5. Solid-state structure of $[(4\text{-}4'\text{-bipy})Ba\{Py_2P(NSiMe_3)_2\}_2]_n$ (**3**). Anisotropic displacement parameters are depicted at the 50% probability level. Selected bond lengths [pm] and angles [deg] are presented in Table 1.

Two pyridyl groups (one each from each ligand) that are cisoid form an acute angle (N21−Sr1−N31 75.22(14)°) when coordinated to strontium. The Sr−N distances (Sr1−N21 269.6(5) and Sr1−N31 268.4(3) pm) are slightly longer than the strontium amide bond distances, as expected. The two remaining pyridyl rings also coordinate in a cisoid manner to the metal center, but in contrast, the angle they form on coordination to the metal ion is twice as wide (N11−Sr1−N41 142.18(13)°). Also the $M-N_{py}$ distances involved (Sr1−N11 287.5(4) and Sr1−N41 281.4(4) pm) are longer than observed with the other pyridyl groups. This coordinating situation enables the seventh coordinating moiety in the form of a solvent THF molecule to approach the metal ion comfortably to complete the hepta-coordination envelope around the strontium ion by fitting in perfectly between the two pyridyl groups (N11−Sr1−O51 72.55(13) and N41−Sr1−O51 71.95(13)°). Although there is no space to accommodate a second THF molecule as at the hexa-coordinated strontium atom in $[(THF)_2Sr\{(NSiMe_3)_2PPh_2\}_2]$,[10] the coordination number increases in **2**.

X-ray Crystal Structure of $[(4,4'\text{-bipy})Ba\{Py_2P(NSiMe_3)_2\}_2]_n$ (3). The barium complex derived from the aminoiminophosphorane **1** was isolated as compound **3** in the presence of the added neutral Lewis base 4,4′-bipyridine. The compound could be crystallized from a mixture of toluene and tetrahydrofuran at −30 °C. Unfortunately, various attempts to crystallize the complex as a THF adduct like **2** valid. Addition of 2,2′-bipyridine was not successful either. The molecule crystallizes in the space group *C*2/*c*. The barium ion and the middle point of the C−C bond of the bipyridine moiety lie on a center of symmetry. Like in **2** the $Py_2P(NSiMe_3)_2$ anions act as tripodal ligands. Two of them are involved in coordination to the barium ion in a similar manner as observed for the strontium complex **2** (Figure 5).

The 4,4′-bipyridine ligands, on the other hand, assist the formation of a polymeric zigzag structural arrangement of **3** (Figure 6).

Thus, each barium ion in the polymeric chain is eight-coordinate. An interesting feature of the polymeric structure of **3** is that the two bipyridine ligands around each barium ion are not *exactly* opposite to each other. Such an arrangement would have led to a linear polymeric structure. Instead in the observed arrangement the N5A−Ba−N5 angle is substantially more acute (125.71(10)°) and leads to the organization of the molecules

(20) Jeffrey, G. A.; Saenger, W. In *Hydrogen Bonding in Biological Structures*; Springer-Verlag: Heidelberg, 1991.

(21) Westerhausen, M.; Schwarz, W. *Z. Anorg. Allg. Chem.* **1991**, *606*, 177.

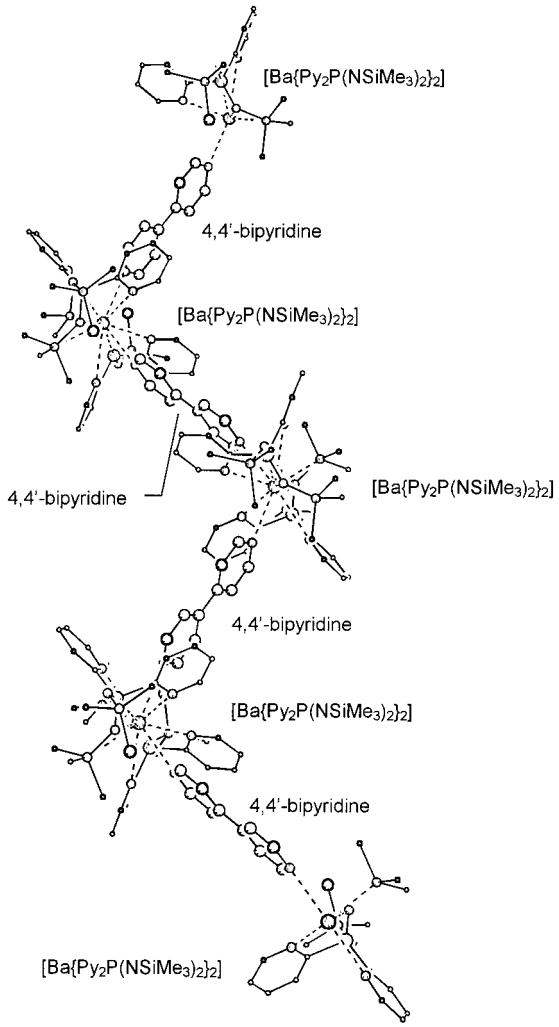

Figure 6. Polymeric zigzag arrangement of [(4,4′-bipy)Ba{Py_2P-$(NSiMe_3)_2\}_2]_n$ (**3**).

into a zigzag-type architecture. The angles between the plane of the bipyridyine motifs and the barium atom are 103.3°(Ba1-4,4′-bipyridine plane) and 76.7° (Ba1A-4,4′-bipyridine plane).

The barium−amido nitrogen distance Ba1−N1 found in **3** is 284.5(2) pm. This value is longer than that observed for other Ba−N covalent bonds found for example in $[(THF)_2Ba\{N(SiMe_3)_2\}_2]$[14,22] (between 259.6(6) and 258.7(6) pm) but only slightly longer than in $[(THF)_2Ba\{(NSiMe_3)_2PPh_2\}_2]$[10] (av 278.3(2) pm). Consistent with the delocalization of the negative charge in the N−P−N segment the two P−N and the two Si−N distances found in **3** are almost equal (P1−N1 158.1(2), P1−N2 156.2(2), Si1−N1 169.9(2), Si2−N2 168.4(2) pm). The two $Ba-N_{py}$ bonds, however, differ considerably by 27.5 pm. The shorter $Ba-N_{py}$ bond length (Ba1−N3) is 285.1(2) pm (which is only slightly longer than the $Ba-N_{amido}$ bond length) whereas the longer bond length (Ba1−N4) is 312.6(2) pm. Although this bond is even longer than the Ba−(η^2)N distance in $[Ba(pz^*_3Ge)_2]$[23] (av 295.0(4) pm) it has to be regarded a donor bond. The short Ba1−N3 bond suggests that the negative charge is delocalized not only in the N−P−N segment of the aminoiminophosphoronate motif (one front of the Janus face) but also extends to include one of the pyridyl substituent at the phosphorus atom (second front of the Janus face).

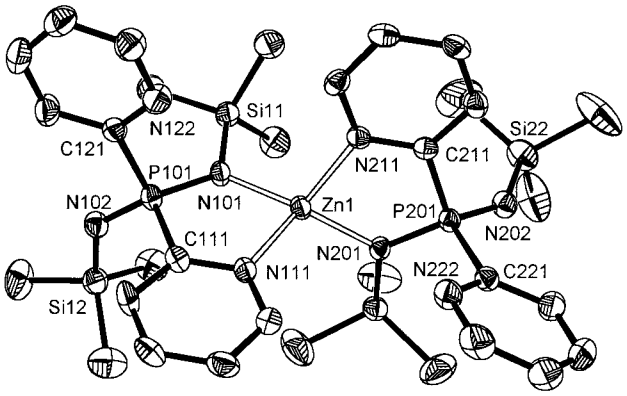

Figure 7. Solid-state structure of $[Zn\{Py_2P(NSiMe_3)_2\}_2]$ (**4**). Anisotropic displacement parameters are depicted at the 50% probability level. Selected bond lengths [pm] and angles [deg] are presented in Table 1.

X-ray Crystal Structure of $[Zn\{Py_2P(NSiMe_3)_2\}_2]$ (4). The molecular structure of the zinc metallacycle **4** is shown in Figure 7.

Unlike compounds **2** and **3** where the metal ions contain ancillary ligands also, the coordination environment of zinc in **4** is entirely made up of two pyridyl aminoiminophosphoronate ligands. Also unlike in **2** and **3**, the $Py_2P(NSiMe_3)_2$ anions function as a bidentate chelating ligand toward the zinc ion. One of the pyridyl nitrogen atoms and the amido nitrogen atom of the pyridyl aminoiminophosphoronate ligands are involved in coordination. Thus, the coordination around zinc is entirely composed of nitrogen atoms and the coordination geometry is approximately tetrahedral with the angles around zinc varying from 90.37(13)° (N201−Zn1−N211) to 136.41(14)° (N101−Zn1−N201). The two Zn−N bond distances corresponding to the amido nitrogen atoms are 197.0(3) (Zn1−N101) and 195.9-(2) pm (Zn1−N201). These values are similar to the one found in the zinc cyclophosphazene, $[N\{P(NMe_2)_2NSiMe_3\}_2ZnN(SiMe_3)_2]$[24] where the corresponding $Zn-N_{amido}$ distance was found to be 198.4(2) pm. However, they are notably longer than Zn−N bonds in zinc amides such as $[Zn\{N(SiMe_3)_2\}_2]$ (182 pm in the gas phase).[25] In **4** the $Zn-N_{py}$ distances are longer than the amido distances: Zn1−N111 206.2(3) and Zn1−N211 208.4(3) pm. These values are comparable to other coordinating distances found for Zn-pyridine complexes.[26] In the dimer $[MeZnC(H)Py_2]_2$ the average $Zn-N_{py}$ distance is 204.0(2) pm.[27] The P−N bond distances in **4** are dissimilar with $P-N_{amido}$ distances (P101−N101 and P201−N201) corresponding to an average value of 161.6(3) pm and $P-N_{imino}$ distances (P101−N102 and P202−N202) averaging to 154.2(4) pm. Obviously metal coordination elongates the P−N distance as in the sidearm donating metalated iminophosporanes $[M(o\text{-}C_6H_4PPh_2NSiMe_3)_2]$; M = Zn[28] 157.4(4), M = Sn[29] 157.3(3), M = Pb[29] 157.0(5) pm in comparison to the parent iminophosporane $Ph_3PNSiMe_3$ (154.2(2) pm).[30] The dissimilarities within the P−N and the

(22) Vaarstra, B. A.; Huffman, J. C.; Streib, W. E.; Caulton, K. G. *Inorg. Chem.* **1997**, *36*, 5140.
(23) Steiner, A.; Stalke, D. *Inorg. Chem.* **1995**, *34*, 4846.
(24) Pandey, S. K.; Steiner, A.; Roesky, H. W.; Stalke, D. *Inorg. Chem.* **1993**, *32*, 5444.
(25) Haaland, A.; Hedberg, K.; Power, P. P. *Inorg. Chem.* **1984**, *23*, 1972.
(26) Review: Haaland, A. *Angew. Chem.* **1989**, *101*, 1017; *Angew. Chem., Int. Ed. Engl.* **1989**, *28*, 992.
(27) Gornitzka, H.; Hemmert, C.; Bertrand, G.; Pfeiffer, M.; Stalke, D. *Organometallics* **2000**, *19*, 112.
(28) Wingerter, S.; Gornitzka, H.; Bertrand, G.; Stalke, D. *Eur. J. Inorg. Chem.* **1999**, 173.
(29) Wingerter, S.; Gornitzka, H.; Bertermann, R.; Pandey, S. K.; Rocha, J.; Stalke, D. *Organometallics* **2000**, *19*, 3890.
(30) Weller, F.; Kang, H.-C.; Massa, W.; Rübenstahl, T.; Kunkel, F.; Dehnicke, K. *Z. Naturforsch., B: Chem. Sci.* **1995**, *50*, 1050.

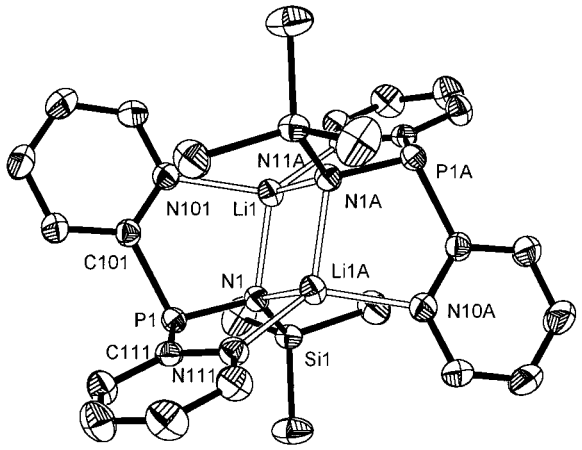

Figure 8. Solid-state structure of $[Li(Py_2PNSiMe_3)]_2$ (**5**). Anisotropic displacement parameters are depicted at the 50% probability level. Selected bond lengths [pm] and angles [deg] are presented in Table 1.

Zn−N distances indicate that in **4** the anionic charge is less delocalized in comparison to the situation observed in **3**.

Crystal Structure of $[Li(Py_2PNSiMe_3)]_2$ (5). The compound **5** is a dimer of the lithium salt of di(2-pyridyl)phosphinotrimethylsilylamine (see Figure 8). The structure of **5** is built around a Li_2N_2 core the ubiquitous structural motif found in lithium amides.[31] Apart from the Li_2N_2 four-membered ring, the structure consists of four five-membered metallacycles. Both the lithium ions are tetracoordinate as a result of coordination of two chelating Py−P−N($SiMe_3$) moieties. This emphasizes the clear preference of the $Py_2P(NSiMe_3)_2$ anion for the involvement of the pyridyl nitrogen atom in conjunction with the amido nitrogen for coordination.[32] The bond-angles within the four-membered Li_2N_2 ring are larger around lithium (104.40(11)°) and smaller around nitrogen (75.60(11)°). The Li−N bond distances within the ring are 206.1(3) pm (Li1−N1) and 206.8(3) pm (Li−N1A). The Li−N_{py} distances are slightly shorter, 202.8(3) pm (Li1−N2) and 203.8(3) pm (Li1−N3A).

The P−N bond distance in **5** is 165.82(12) pm which is longer than the P═N double bond values found for iminophosphoranes (147−162 pm),[33] but it is comparable to the P−N distance found in $[(Et_2O)Li(PhNPPh_2)]_2$ [34] (167.2(2)pm) and in $[(THF)_3Na(Ph_2PNSiMe_3)]$[35] (163.6(8) pm).

Structural Comparison between 2, 3, and 4. It is interesting to note that in the complexes **2**, **3**, and **4** the dipyridylaminoiminophosphoronate $Py_2P(NSiMe_3)_2$ ligand utilizes at least one pyridyl ligand in conjunction with an amido nitrogen for coordination. Even in the lithium complex **5**, although the ligand is now truncated, a similar mode of coordination is seen. This reactivity behavior distinguishes it from the diphenylaminoiminophosphoronate ligand $Ph_2P(NSiMe_3)_2$ which in its reactivity acts as a $[NPN]^-$ ligand exclusively. Presumably the reason for the different reactivity of **1** stems from the possibility of greater stability associated with a five-membered metallacycle that is formed by involving the pyridyl nitrogen atom in preference to the four-membered metallacyle formation that would occur if the imino nitrogen and the amido nitrogen atoms coordinate together. With barium and strontium ions which have a preference for larger coordination numbers deprotonated **1** acts as a tripodal ligand utilizing both the pyridyl groups and the amido nitrogen atom. However, zinc which prefers a tetrahedral geometry with four ligands solicits and obtains a bidentate chelating mode from $Py_2P(NSiMe_3)_2^-$. These varied modes of coordination point to the flexible nature of the multidentate ligand.

The various structural parameters of compounds **1**−**4** are summarized in Table 1. The first point of interest is the variation and the difference in the two P−N bond lengths in the $Py_2P(NSiMe_3)_2$ moiety in the compounds **1**−**4**. The largest difference is quite obviously in the native ligand containing the amino hydrogen atom (**1**). The P−N bond lengths here differ by 12.0 pm with the shorter bond length being 152.9(2) pm. This represents one extreme of the situation in which there is a more localized structure in terms of the P−N double and single bonds. As the amino group is deprotonated and the ligand is involved in the formation of the metallacycle, the difference in the P−N bond lengths decreases. This is indicative of a growing delocalization of the negative charge over the entire fragment (Figure 9).

A near complete delocalization is realized in the barium complex **3** where both the P−N bonds have nearly equal distance and the difference between them reduces to only 1.9 pm. The situation with the zinc complex **4** and the strontium complex **2** is intermediate in nature with the former closer to the ligand ($\Delta_{P-N} = 7.6$ pm) and the latter to that of the barium complex ($\Delta_{P-N} = 4.3$ and 5.1 pm). A similar trend is also noticeable in the two Si−N bond distances found for these compounds. Thus, in **1** the Δ_{Si-N} is 7.3 pm and it progressively decreases in **4** (6.2 and 2.4 pm), **2** (4.4 and 3.7 pm), and **3** (1.5 pm), consistent with the trend found in the P−N bond lengths. In contrast to these changes the P−C bonds remain completely unaffected from **1** through **4**. The bond angle variations, although smaller in magnitude in comparison to the bond length changes, also are consistent with the above arguments. It can be seen that the N−P−N angle widens upon metal coordination with the highest value being observed for the barium complex **3** (125.79(12)°). The C−P−C angles shrink upon coordination although the magnitude of change is only marginal. An interesting correlation is observed between the P−N_{coord}−Si bond angle and the corresponding P−N bond. As the bond angle increases the P−N bond length decreases.

Conclusions

Substitution of the organic alkyl or aryl groups in the classical $NP(R_2)N^-$ chelating anionic ligand by two pyridyl groups converts it into a Janus face $NP(Py_2)N^-$ tripodal ligand. At least one pyridyl ring nitrogen in addition to only one imido nitrogen atom is used in metal coordination. The active ligand periphery opens up several avenues: (a) coordination site selectivity NPN^- versus PyPPy, (b) adaptability in ligation composition, depending on the geometric constraints and coordination capability of the metals, and (c) the possibility of forming heterobimetallic complexes where the dipyridyl aminoiminophophoranes are employed as flexible metal linkers and not only as bulky protectants. Surprisingly, in pyridyl-substituted aminoiminophophoranes it is easy to cleave either one or both P−N bonds. This reduction of P(V) species to P(III) compounds is very uncommon and supplies easy access to phosphanylamines and secondary phosphanes, not easy to make by different routes.

(31) (a) Armstrong, D. R.; Barr, D.; Clegg, W.; Mulvey, R. E.; Reed, D.; Snaith, R.; Wade, K. *J. Chem. Soc., Chem. Commun.* **1986**, 869. Reviews: (b) Gregory, K.; Schleyer, P. v. R.; Snaith, R. *Adv. Inorg. Chem.* **1991**, *37*, 47. (c) Mulvey, R. E. *Chem. Soc. Rev.* **1991**, *20*, 167. (d) Mulvey, R. E. *Chem. Soc. Rev.* **1999**, *27*, 339.

(32) Steiner, A.; Stalke, D. *Angew. Chem.* **1995**, *107*, 1908; *Angew. Chem., Int. Ed. Engl.* **1995**, *34*, 1752.

(33) Review: Niecke, E.; Gudat, D. *Angew. Chem.* **1991**, *103*, 251; *Angew. Chem., Int. Ed. Engl.* **1991**, *30*, 217

(34) Ashby, M. T.; Li, Z. *Inorg. Chem.* **1992**, *31*, 1321.

(35) Wingerter, S.; Pfeiffer, M.; Baier, F.; Stey, T.; Stalke, D. *Z. Anorg. Allg. Chem.* **2000**, *626*, 1121.

Table 1. Selected Bond Lengths [pm] and Angles [deg] in **1**−**5**

	1 ('M′ = H)	**2** (M = Sr)		**3** (M = Ba)	**4** (M = Zn		**5** (M = Li
$P-N_{M-coord}$	164.9(2)	158.2(4)	159.3(4)	158.1(2)	161.9(3)	161.2(3)	165.82(12)
$P-N_{not\ M-coord}$	152.9(2)	153.9(4)	154.2(5)	156.2(2)	154.8(4)	153.6(3)	–
$P-C_{Pyridyl,\ not\ M-coord}$	183.0(2)	–	–	–	182.7(4)	183.9(4)	–
$P-C_{Pyridyl,\ M-coord}$	182.4(2)	184.9(6)	183.1(6)	186.0(3)	185.0(4)	183.8(4)	185.8(2)
		184.5(6)	184.3(6)	183.9(2)			186.5(2)
$N_{not\ M-coord.}$-Si	168.1(2)	166.2(4)	165.5(5)	168.4(2)	171.2(4)	167.5(3)	–
$N_{M-coord.}$-Si	175.4(2)	169.9(4)	169.4(5)	169.9(2)	173.6(3)	173.7(3)	171.33(12)
$M-N_{N-P}$	80.7(2)	260.6(4)	259.3(4)	284.5(2)	197.0(3)	195.9(3)	206.1(3)
							206.8(3)
$M-N_{Pyridyl}$	321.3(2)	269.9(5)	268.4(5)	285.1(2)	206.2(3)	208.4(3)	202.8(3)
		287.5(4)	281.4(4)	312.6(2)			203.8(3)
N−P−N	111.94(9)	122.3(2)	124.4(3)	125.79(12)	123.3(2)	123.0(2)	–
C−P−C	101.53(8)	99.0(2)	97.7(2)	98.40(11)	100.5(2)	100.1(2)	97.15(7)
$P-N_{M-coord}-Si$	123.10(10)	127.0(2)	126.9(3)	127.73(14)	125.0(2)	122.5(2)	114.73(7)
$P-N_{not\ M-coord}-Si$	146.89(11)	163.3(3)	173.3(4)	135.01(14)	133.1(2)	141.9(2)	–

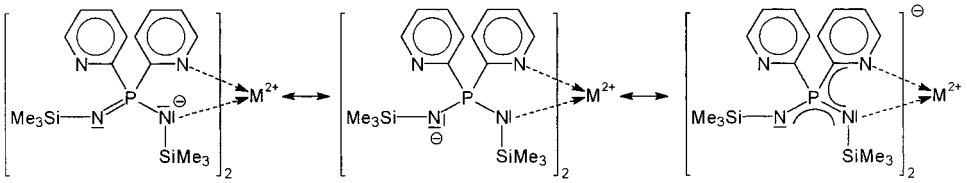

Figure 9. Various resonance forms of the dipyridyl aminoiminophoshoranate anion depicting different delocalization moieties.

Experimental Section

All manipulations were performed under inert gas atmosphere of dry N_2 with Schlenk techniques or in an argon glovebox. All solvents were dried over Na/K alloy and distilled prior to use. NMR spectra were obtained in benzene-d_6 or toluene-d_8 as solvent with $SiMe_4$ or H_3PO_4 as external reference on a Bruker AM 250. Mass spectra were recorded on a Finnigan Mat 8230 or Varian Mat CH5 spectrometer. Elemental analyses were performed by the Analytische Laboratorium des Instituts für Anorganische Chemie der Universität Würzburg.

Di(2-pyridyl)phosphane[16] and alkalineearthbis(bis(trimethylsilyl))-amides[14,21] were prepared according to known literature procedures. Syntheses of the other compounds reported in this paper are carried out as per the procedures given below.

$Py_2P\{N(H)SiMe_3\}(NSiMe_3)$ (1). Di(2-pyridyl)phosphane (2.80 g, 14.9 mmol) and trimethylsilyl azide (4.29 g, 32.8 mmol) were taken together and stirred at 25 °C for 1 day. After this the reaction mixture was heated under reflux for 5 days. The orange residue was stripped of the excess of trimethylsilyl azide in a vacuum. Also, 4,4′-bipyridine that was formed in the reaction was removed by vacuum sublimation at 60 °C. The remaining product was distilled in a vacuum to obtain an orange-red oil (110 °C at 0.01 Torr). After a few days colorless crystals were obtained from the above oil which were suitable for single-crystal X-ray analysis. Treatment of the remaining oil with a mixture of toluene and pentane (5:1) and cooling this mixture at −30 °C afforded a white solid. 1.28 g. The mother liquor was stripped off, the solvent was removed in a vacuum, and the residue was treated again with pentane (10 mL) to obtain a further crop of 0.82 g. Overall Yield: 39%; mp 58−64 °C. ^{1}H NMR (C_6D_6): δ = 0.13 (s, 9H,$SiMe_3$), 0.38 (s, 9H, $SiMe_3$), 4.72 (s,1H, N−H), 6.45 (m, 2H, 5-H_{py}), 6.98 (m, 2H, 4-H_{py}), 8.05 (ddd, $^3J_{3,4}$ = 7.8 Hz, $^3J_{3,5}$ = 6.4 Hz,$^5J_{3,6}$ = 1.1 Hz, 2H, 3-H_{py}), 8.26 (d, $^3J_{6,5}$ = 4.8 Hz, 2H, 6-H_{py}); ^{13}C NMR (C_6D_6): δ = 2.1 (s, $SiMe_3$), 124.0−135.6 (m, Py-C), 149.3 (d, $^3J_{C,P}$ = 26.8 Hz, 6-C), 158.5 (d, $^1J_{C,P}$ = 120.7 Hz, 2-C); ^{29}Si NMR (toluene-d_8): δ = 6.6 and 7.3; ^{31}P NMR (toluene-d_8): δ = −6.2; IR (Nujol, KBr): ν [cm^{-1}] = 3355 (N−H), 1600, 1479, 1454, 1273, 1263, 1194, 1150, 1100, 1040, 985; MS(70 eV) *m*/*z*(%): 348(0.2) [M^+ − Me], 147 (100%), $[(C_4H_3)_2PN]^+$. Anal. Calcd for $C_{16}H_{27}N_4PSi_2$: C: 54.4; H: 6.66; N: 15.1. Found: C: 53.4; H: 6.34; N: 16.5.

$[(THF)Sr\{Py_2P(NSiMe_3)_2\}_2]$ (2). A solution of $[(THF)_2Sr\{N(SiMe_3)_2\}_2]$ (2.50 mmol) in 10 mL of hexane was added to **1** (1.80 g, 5.0 mmol) in 10 mL of hexane, and the reaction mixture was stirred for 48 h. A precipitate that had formed in the reaction was filtered and recrystallized from THF/pentane at room temperature. 1.25 g, 56.8%; mp 55 °C (dec). ^{1}H NMR (C_6D_6): δ = 0.47 (s, 18H, $SiMe_3$), 3.59 (m, 4H, THF), 6.90−8.60 (m, 8H, Py-H) ^{31}P NMR (C_6D_6): δ = −15.9(s); MS(70 eV) *m*/*z*(%): 810(40) [M − THF]$^+$. Anal. Calcd for $C_{36}H_{60}N_8OP_2Si_4Sr$: C: 48.9; H: 6.85; N: 12.7. Found: C: 47.5; H: 6.92; N: 12.6.

$[(4,4'\text{-bipy})Ba\{Py_2P(NSiMe_3)_2\}_2]_n$ (3). A mixture of **1** (1.81 g, 4.99 mmol), 4,4′-bipyridine (0.39 g, 2.50 mmol), and $[(THF)_2Ba\{N(SiMe_3)_2\}_2]$ (1.51 g, 2.50 mmol) in toluene (10 mL) were stirred together at −78 °C. The solution was clear and yellowish in color. It was stirred at −78 °C for 2 h, allowed to warm to room temperature, and stirred overnight. A white solid which was precipitated was filtered and dried in a vacuum. 1.55 g, 61%; mp 204 °C (DTA). ^{1}H NMR (THF-d_8): δ = 0.19 (s, 18H, $SiMe_3$), 0.27 (s, 18H, $SiMe_3$), 6.84−8.67 (m, 24 H, Py-H). ^{31}P NMR (THF-d_8): δ = −4.3; IR: ν [cm^{-1}] = 2834, 1300, 1257, 1217, 1151, 1095, 1026, 1010, 952; MS(70 eV) *m*/*z*(%): 347-(100) $[Py_2P(NSiMe_3)(NSiMe_2)]^+$. Anal. Calcd for $C_{42}H_{60}BaN_{10}P_2Si_4$: C: 49.6; H: 5.95; N: 13.8. Found: C: 50.9; H: 6.08; N: 13.1.

$[Zn\{Py_2P(NSiMe_3)_2\}_2]$ (4). To a solution of **1** (0.50 g, 1.38 mmol) in pyridine (5 mL) was added under stirring at room temperature a solution of dimethylzinc (0.34 mL, 0.69 mmol) (2.0 M in toluene). The color of the reaction mixture became yellow. It was stirred for 4 h and left at room temperature. After a few hours single crystals suitable for X-ray diffraction grew from the solution. They were filtered, and the mother liquor was dried in a vacuum to obtain a white residue. It was washed with pentane (10 mL) and dried in a vacuum. The crystals as well as the product obtained from the mother liquor were found to be the same and corresponded to the title compound. 0.50 g, 46%; mp 142 °C. ^{1}H NMR (C_6D_6): δ = 0.30 (s, 18H, $SiMe_3$), 0.50 (s, 18H, $SiMe_3$), 6.40−7.25(m, 8H, Py-H), 8.00−9.00 (m, 8H, Py-H); ^{13}C NMR (C_6D_6): δ = 2.7 (s, $SiMe_3$), 3.6 (s, $SiMe_3$), 122.4−135.7 (m, Py-C), 146.9 (d, $^3J_{C,P}$ = 18.1 Hz, 6-C). (2-C not detected); ^{29}Si NMR (C_6D_6): δ = −21.7; ^{31}P NMR (C_6D_6): δ = −3.5; IR (Nujol, KBr): ν [cm^{-1}] = 2881, 1510, 1265, 1232, 1154, 1108, 1090, 1041, 1030, 999, 857; MS(70 eV) *m*/*z*(%): 788(4) [M]$^+$, 347(100) $[Py_2P(NSiMe_3)(NSiMe_2)]^+$. Anal. Calcd for $C_{32}H_{52}N_8P_2Si_4Zn$: C: 48.8; H: 6.65; N: 14.2. Found: C: 47.2; H: 6.59; N: 14.3.

$[Li(Py_2PNSiMe_3)]_2$ (5). To a solution of **1** (1.00 g, 2.76 mmol) in THF (10 mL) was added under stirring at room temperature a solution of $[(THF)LiN(SiMe_3)_2$ (0.66 g, 2.76 mmol) in 10 mL of THF. The color of the reaction mixture became red. It was stirred for 2 d and stored at −30 °C. After a further 2 d single crystals suitable for X-ray

Table 2. Crystallographic Data for **1**−**5** at 173 K

	1	**2**	**3**	**4**	**5**
empirical formula	$C_{16}H_{27}N_4PSi$	$C_{36}H_{60}N_8OP_2Si_4Sr + C_4H_8O + C_5H_{12}$	$C_{42}H_{60}BaN_{10}P_2Si_4$	$C_{32}H_{52}N_8P_2Si_4Zn$	$C_{26}H_{34}Li_2N_6P_2Si_2$
CCDC-number	151948	151949	151950	151951	151952
formula weight	362.57	1027.09	1016.64	788.49	562.59
crystal size [mm]	0.6 × 0.5 × 0.4	0.6 × 0.6 × 0.2	0.3 × 0.3 × 0.2	0.4 × 0.3 × 0.2	0.6 × 0.4 × 0.4
crystal system	monoclinic	monoclinic	monoclinic	triclinic	monoclinic
space group	$P2_1/c$	$P2_1/c$	$C2/c$	$P\bar{1}$	$C2/c$
a [pm]	944.8(2)	2274.9(2)	3003.1(6)	960.4(3)	1921.5(2)
b [pm]	987.5(2)	1412.8(2)	917.0(2)	1499.9(4)	1077.37(11)
c [pm]	2225.1(5)	1905.6(2)	2160.2(4)	1591.8(4)	1537.2(2)
α [deg]	90	90	90	109.03(2)	90
β [deg]	91.97(3)	106.521(10)	124.51(3)	102.29(2)	99.767(14)
γ [deg]	90	90	90	99.34(2)	90
V [nm^{-3}]	2.0749(7)	5.8717(10)	4.902(2)	2.0505(10)	3.1361(6)
Z	4	4	4	2	4
ρ_c [Mg m^{-3}]	1.161	1.162	1.377	1.277	1.192
μ_c [mm^{-1}]	0.252	1.093	1.014	0.827	0.240
F(000)	776	2184	2096	832	1184
2θ range [deg]	4.52−50.70	5.00−41.00	4.74−50.70	6.14−45.12	5.30−50.70
no. reflns. measd.	16561	20646	22640	6434	20490
no. unique reflns.	3794	5951	4482	5288	2861
no. of restraints	0	657	48	0	0
no. of parameters	218	663	305	436	176
$R1$[a]) [$I > 2\sigma(I)$]	0.0350	0.0456	0.0278	0.0417	0.0307
$wR2$[b]) (all data)	0.0940	0.0911	0.0740	0.1182	0.0839
g_1; g_2c)	0.0563; 0.4355	0.0390; 8.0000	0.0509; 4.0504	0.0604; 3.8963	0.0563; 0.4355
largest diff. peak and hole (e nm^{-3})	329 and −216	427 and −297	1233 and −611	625 and −720	329 and −216

[a] $R1 = \sum||F_o| - |F_c||/\sum|F_o|$. [b] $wR2 = \sqrt{\sum w(F_o^2-F_c^2)^2/\sum w(F_o^2)^2}$. [c] $w = 1/\sigma^2(F_o^2) + (g_1P)^2 + g_2P$; $P = (\max(F_o^2,0) + 2F_c^2)/3$.

diffraction were obtained from the solution. They were filtered, washed with pentane (10 mL), and dried in a vacuum. 0.48 g, 62%; mp 266 °C. ^{1}H NMR (C_6D_6): $\delta = 0.54$ (s, 18H, $SiMe_3$), 6.40−8.70 (m, 16H, Py-H); ^{7}Li NMR (C_6D_6): $\delta = 4.1$; ^{13}C NMR (C_6D_6): $\delta = 4.57$ (s, $SiMe_3$), 122.1−165.0 (m, Py-C); ^{31}P NMR (C_6D_6): $\delta = 15.3$; IR (Nujol, KBr): ν [cm^{-1}] = 1489, 1312, 1166, 1109, 1087, 1944, 1013, 976; MS (70 eV) m/z(%): 281(0.2) $[LiPy_2PNSiMe_3]^+$, 260(80) $[Py_2P(NSiMe_2)]^+$, 182(100) $[PyP(NSiMe_2)]^+$. Anal. Calcd for $C_{26}H_{34}Li_2N_6P_2Si_2$: C: 55.5; H: 6.09; N: 14.9. Found: C: 55.3; H: 6.17; N: 14.5.

[(THF)$_2$Li(Py$_2$P)] (6). To a solution of **1** (1.00 g, 2.76 mmol) in THF (15 mL) an equimolar solution of *n*-butyllithium (1.72 mL, 2.76 mmol, 1.6 M in hexane) or methyllithium (1.72 mL, 2.76 mmol, 1.6 M in Et_2O) was added under stirring at −78 °C. It was allowed to warm to room temperature and stirred for a further 2 d. The color of the reaction mixture turned red. The mixture was stored at −18 °C and after 3 d single crystals suitable for X-ray diffraction were obtained from the solution. They were filtered, washed with pentane (10 mL), and dried in a vacuum. 0.63 g, 68%. The analytical data of **6** do not differ from those of [(THF)$_2$Li(Py$_2$P)] obtained from the reaction of Py_2PH and *n*-butyllithium communicated earlier.[16b]

X-ray Measurements of 1−5. All data were collected from shock-cooled crystals[36] at 173(2) K on a Stoe IPDS one circle diffractometer (compounds **1**, **2**, **3**, and **5**) or on an Enraf-Nonius CAD4 four-circle diffractometer (compound **4**) (graphite-monochromated Mo Kα radiation, $\lambda = 71.073$ pm) equipped with a low-temperature device. All structures were solved by direct methods (SHELXS-97)[37] and refined by full-matrix least-squares methods against F^2 (SHELXL-97).[38] All non-hydrogen atoms were refined with anisotropic displacement parameters. Hydrogen atoms bonded to nitrogen atoms were located by difference Fourier syntheses and refined isotropically with N−H distance restraints. All other hydrogen atoms of the molecules were assigned ideal positions and refined isotropically using a riding model with U_{iso} constrained to 1.2 times the U_{eq} of the parent atom. In **2** the noncoordinated THF and pentane were disordered and refined to a split occupancy of 0.61/0.39 for the THF and 0.57/0.43 for the pentane, respectively, using distance and similarity restraints. In **3** the Me_3Si-group for Si2 was disordered and refined to a split occupancy of 0.85/0.15, employing distance and similarity restraints. Selected bond lengths and angles are summarized in Table 2. Other crystallographic data (excluding structure factors) for the structures reported in this paper have been deposited with the Cambridge Crystallographic Data Center as supplementary publication (CCDC numbers see Table 2). Copies of the data can be obtained free of charge on application to CCDC, 12 Union Road, Cambridge CB2 1EZ, UK [Fax: (international) + 44-(1223)336-033; e-mail: deposit@ccdc.cam.ac.uk].

Acknowledgment. We thank the Deutsche Forschungsgemeinschaft, the Würzburger Sonderforschungsbereich 347, the Fonds der Chemischen Industrie, the DAAD, and the Alexander von Humboldt Stiftung for financial support. D.S. kindly acknowledges support of Bruker axs-Analytical X-ray Systems, Karlsruhe, and CHEMETALL, Frankfurt/Main.

Supporting Information Available: Tables of crystal data, fractional coordinates, bond lengths and angles, anisotropic displacement parameters, and hydrogen atom coordinates of the structures **1**−**5** (PDF). This material is available free of charge via the Internet at http://pubs.acs.org.

JA0023736

(36) Stalke, D. *Chem. Soc. Rev.* **1998**, *27*, 171.
(37) Sheldrick, G. M. *Acta Crystallogr., Sect. A* **1990**, *46*, 467.
(38) Sheldrick, G. M. *SHELXL-97*, Program for Crystal Structure Refinement; University of Göttingen, Göttingen, Germany, 1997.